Pharmaceutical Sciences and Drug Design
ISSN: 3062-4428
2026, Volume 6, Issue 1, Page No: 119-133

Available online at: www.galaxypub.co/page/journals

Galaxy Publication

Galaxy Publication

Circulating miRNAs as Predictive Biomarkers of Cardiotoxicity in HER2-Positive Breast Cancer: A Prospective Clinical Study

Maria Hernandez[1]*, Carlos Vega[1]

[1]Department of Pharmaceutical Sciences and Therapeutic Design, Faculty of Pharmacy, University of Valencia, Valencia, Spain.

***E-mail** ✉ maria.hernandez@gmail.com

Received: 01 December 2025; **Revised:** 02 March 2026; **Accepted:** 06 March 2026

ABSTRACT

Individuals with HER2-positive breast cancer treated with chemotherapy and targeted agents, such as anthracyclines and trastuzumab, are at heightened risk of developing cardiotoxic effects that may progress to long-term cardiovascular complications. Early identification of predictive biomarkers is therefore critical for timely clinical intervention. Circulating microRNAs (miRNAs), which regulate gene expression and play important roles in cardiovascular biology, have recently been proposed as potential indicators of cardiotoxicity. This study investigates alterations in circulating miRNA expression in HER2-positive breast cancer patients receiving chemotherapy and assesses their ability to predict treatment-related cardiotoxicity using machine learning. A total of forty-seven patients were followed for cardiac toxicity assessment at baseline and every 3 months for a period of up to 15 months. Baseline peripheral blood samples were obtained. Expression profiling of 84 microRNAs was conducted using the miRCURY LNA miRNA PCR Panel. Relative expression differences were calculated using the $2^{-\Delta\Delta Ct}$ method. The five most significantly upregulated and five most downregulated miRNAs were subsequently evaluated using univariate logistic regression and receiver operating characteristic (ROC) curve analysis. Five machine learning algorithms (Decision Tree, Random Forest (RF), Support Vector Machine (SVM), Gradient Boosting Machine (GBM), and k-Nearest Neighbors (KNN)) were developed to classify cardiotoxicity based on miRNA expression patterns. A total of forty-five miRNAs demonstrated significant differential expression between patients with and without cardiotoxicity. ROC analysis identified hsa-miR-155-5p (AUC 0.76, $p = 0.006$) and hsa-miR-124-3p (AUC 0.75, $p = 0.007$) as the most powerful individual predictors. The kNN, SVM, and RF models achieved high predictive performance. The decision tree approach highlighted hsa-miR-17-5p and hsa-miR-185-5p as key discriminative features. Both SVM and RF models revealed additional cardiotoxicity-associated miRNAs (SVM: hsa-miR-143-3p, hsa-miR-133b, hsa-miR-145-5p, hsa-miR-185-5p, hsa-miR-199a-5p; RF: hsa-miR-185-5p, hsa-miR-145-5p, hsa-miR-17-5p, hsa-miR-144-3p, and hsa-miR-133a-3p). Overall evaluation metrics showed that SVM, kNN, and RF outperformed the decision tree model in predictive accuracy. Pathway enrichment analysis of top-ranked miRNAs indicated significant enrichment in apoptosis, p53, MAPK, and focal adhesion signaling pathways, all of which are implicated in chemotherapy-associated cardiac injury and remodeling. Circulating miRNAs may serve as valuable biomarkers for predicting cardiotoxicity in patients with breast cancer. The integration of machine learning approaches can improve miRNA-based risk stratification, supporting personalized surveillance and early cardioprotective interventions.

Keywords: Cardiotoxicity, Breast cancer, Machine learning, MicroRNA, Biomarker

How to Cite This Article: Hernandez M, Vega C. Circulating miRNAs as Predictive Biomarkers of Cardiotoxicity in HER2-Positive Breast Cancer: A Prospective Clinical Study. Pharm Sci Drug Des. 2026;6(1):119-33. https://doi.org/10.51847/LRihQzFRst

Introduction

Anthracyclines and trastuzumab represent cornerstone agents in (neo)adjuvant treatment regimens for human epidermal growth factor receptor 2 (HER2)-positive early breast cancer. Despite their therapeutic effectiveness, both are associated with cardiotoxicity that may culminate in severe myocardial dysfunction and heart failure [1, 2]. When used in combination, these agents are linked to a cardiotoxicity incidence of approximately 27% [3]. As a result, sequential (two-step) administration has been adopted as standard practice over the past two decades,

reducing cardiotoxic events to about 3%–4% [4-6]. Another established mitigation strategy involves limiting anthracycline exposure, with current guidelines recommending a cumulative doxorubicin dose of 400–550 mg/m² to reduce the risk of heart failure [7]. Nevertheless, the most critical challenge remains the early detection and clinical management of cardiotoxicity to prevent irreversible cardiac impairment and preserve quality of life.

Prognostic biomarkers are essential for identifying patients at risk of developing treatment-induced cardiotoxicity. Cardiac troponins, particularly high-sensitivity troponin, and N-terminal pro B-type natriuretic peptide (NT-proBNP) have been extensively investigated as diagnostic and prognostic tools; however, their clinical utility remains inconsistent. Several studies have reported no significant association between these biomarkers and cardiotoxicity [8-10], whereas others have demonstrated a correlation for at least one marker [11-14]. Emerging circulating biomarkers, including myeloperoxidase, soluble ST2, growth differentiation factor 15, and microRNAs, are currently under investigation for their potential roles in detecting and predicting cardiotoxicity. Despite these developments, validated biomarkers for early detection remain lacking, significantly limiting proactive clinical decision-making and individualized risk stratification. This unmet need serves as the basis for the present study and supports the rationale for applying machine learning methodologies to address this gap.

Accordingly, this study evaluates circulating miRNAs as prognostic biomarkers of chemotherapy-induced cardiotoxicity in breast cancer patients treated with epirubicin plus cyclophosphamide, followed by taxane and trastuzumab.

Materials and Methods

Patients and blood samples

A total of 47 patients diagnosed with operable breast cancer were enrolled following surgical resection and before initiation of adjuvant chemotherapy. Treatment consisted of four cycles of epirubicin at 75 mg/m², administered via slow intravenous push over 10–15 minutes, combined with cyclophosphamide at 600 mg/m², administered as a 30–60-minute intravenous infusion every 2 weeks. This regimen was followed by 12 weekly cycles of paclitaxel at 80 mg/m², delivered as a 1-hour intravenous infusion, together with trastuzumab, initially at 8 mg/kg as a 90-minute intravenous infusion and subsequently at 6 mg/kg over 30–90 minutes every 3 weeks. After completion of chemotherapy, trastuzumab was continued every 3 weeks for a total treatment duration of one year.

Peripheral blood samples were collected at baseline, and cardiac toxicity surveillance—including echocardiographic evaluation and arterial blood pressure measurement—was performed every 3 months from treatment initiation until completion of trastuzumab therapy (15 months), in accordance with standard clinical practice and the 2022 ESC cardio-oncology guidelines for high-risk patients [15].

Inclusion criteria consisted of: (1) histologically confirmed HER-2 positive breast cancer; (2) indication for adjuvant chemotherapy including anthracyclines and trastuzumab; and (3) baseline left ventricular ejection fraction (LVEF) above 50%. Exclusion criteria included: (1) systemic inflammatory disease or active infection; (2) hepatic or renal dysfunction; (3) ischemic heart disease or LVEF below 50%; (4) significant structural myocardial disease; and (5) uncontrolled hypertension.

Given the exploratory and pilot nature of the study and the lack of prior robust data to estimate effect sizes for circulating miRNAs in this clinical context, no formal sample size calculation was performed before study initiation. Instead, all consecutively treated and eligible HER2-positive breast cancer patients during the recruitment period with complete clinical data and available biospecimens were included.

All included cases were recruited from the Department of Clinical Therapeutics at the Alexandra Hospital, National and Kapodistrian University of Athens Medical School, over the period from May 2015 to July 2019. Ethical approval was granted by the Ethics Committee of “Hippokration” Athens General Hospital (Approval Code: 8028; Approval Date: 17 June 2015). Before inclusion, every participant signed a written informed consent form, which specifically covered permission for blood sampling and the use of clinical data for research purposes.

Following cardiac evaluation, patients were assigned to either the cardiotoxicity or non-toxicity group. Cardiotoxicity was defined according to the presence of any of the following criteria: symptomatic decline in LVEF; asymptomatic reduction of LVEF to < 40%; a decrease in LVEF ≥ 10% from baseline resulting in values between 40 and 49%; or a < 10% reduction from baseline with LVEF between 40 and 49% accompanied by a > 15% decrease in Global Longitudinal Strain (GLS), or a newly elevated cardiac biomarker profile [high-sensitivity troponin I (hs-TnI) > 15 pg/mL and NT-proBNP > 125 pg/mL]; alternatively, LVEF ≥ 50% combined with a >

15% reduction in GLS and/or newly increased cardiac biomarkers [high-sensitivity troponin I (hs-TnI) > 15 pg/mL and NT-proBNP > 125 pg/mL].

For sample processing, blood was collected in serum separator tubes, allowed to clot for 30 minutes at room temperature, and then centrifuged at 3000 rpm for 10 minutes at 4 °C. Serum aliquots were prepared immediately afterward and stored at −80 °C without undergoing repeated freeze–thaw cycles. All analyses were conducted using identical reagent lots to minimize technical variability.

MiRNA expression

Total circulating RNA was isolated from 300 µL of human serum using the NucleoSpin miRNA Plasma Kit (Macherey-Nagel, Düren, Germany), strictly following the manufacturer's protocol and consistent with a previously established laboratory workflow [16]. RNA quantification was performed using a Qubit Fluorometer (Thermo Fisher Scientific, Waltham, MA, USA), yielding typical concentrations of 25–30 ng/µL in a final elution volume of 20 µL, corresponding to approximately 500–600 ng total RNA per sample.

For reverse transcription, RNA input was standardized to 5 ng/µL according to the miRCURY LNA RT Kit recommendations. Each reaction contained 4 µL of RNA at 5 ng/µL (equivalent to 20 ng total RNA) in a final volume of 20 µL, following the miRCURY LNA Focus Panels protocol for serum/plasma samples. Expression profiling of 84 miRNAs was carried out using the miRCURY LNA miRNA PCR Panel, Human Cardiovascular Disease Focus V2 (Cat. no. YAHS-213Y, Qiagen, Hilden, Germany), together with the miRCURY LNA SYBR Green Master Mix.

Each panel included ten small nucleolar/small nuclear RNA controls for normalization purposes (SNORD44 (hsa), SNORD38B (hsa), SNORD49A (hsa), U6snRNA (v2), UniSP2, UniSP3, UniSP4, UniSP5, UniSP6, and cel-miR-39-3p as an external spike-in control), along with a miRNA reverse transcription control (RTC) and a positive PCR control (PPC). The cel-miR-39-3p spike-in served as a quality control for RNA extraction and reverse transcription efficiency, ensuring comparability across serum samples. Endogenous small RNAs (including SNORD44, SNORD49A, and U6snRNA) were used for normalization using the $2^{-\Delta Ct}$ method.

Samples were categorized into cardiotoxicity and non-toxicity groups. Relative expression levels were calculated for each miRNA using the $2^{-\Delta Ct}$ method according to the miRCURY LNA miRNA PCR Data Analysis platform (https://dataanalysis2.qiagen.com/miRCury, accessed on 24 October 2024). Fold changes between groups were calculated using the 2^−ΔΔCt method and reported as fold regulation in a biologically interpretable format, accompanied by the standard error of the mean (SEM) and 95% confidence intervals (CI).

Statistical comparisons were performed using Student's t-test on replicate-normalized miRNA expression values between cardiotoxicity and non-toxicity groups. Resulting p-values were adjusted for multiple testing using the Benjamini–Hochberg false discovery rate (FDR) correction implemented via the p.adjust function in R.

Machine learning modeling approach

To investigate whether miRNA profiles can predict cardiotoxicity in breast cancer patients treated with targeted therapies, five independent machine learning algorithms were applied. The decision tree classifier was implemented through the rpart package (version 4.1.24) and designed to assign patients to cardiotoxicity or non-toxicity groups based on selected miRNA inputs. The full workflow included preprocessing, handling class imbalance, feature selection, and model development.

To overcome uneven class distribution, we applied the ROSE (Random Over-Sampling Examples) approach. This method generates artificial observations by simultaneously oversampling underrepresented cases and undersampling the dominant class, producing a more balanced dataset and reducing classification bias. After balancing, the dataset was split into training (80%) and testing (20%) subsets using stratified sampling to preserve the original class proportions.

Model performance and stability were evaluated using repeated 10-fold cross-validation (10 repetitions) on the training dataset. In parallel, a Random Forest model was trained to quantify the contribution of each miRNA variable to classification performance. This model was built using 500 decision trees, with 5 variables randomly selected at each node split. Feature relevance was estimated using the Gini impurity criterion, and the highest-ranked miRNAs were visualized through importance plots. The final decision tree was then constructed using the top three miRNAs identified from the Random Forest ranking.

Within the random forest (RF) framework, variable importance was measured using the mean decrease in Gini index via the randomforest package (version 4.7-1.2). This score reflects how much each miRNA improves node purity during splitting, with higher values indicating stronger predictive contribution.

For the linear support vector machine (SVM), feature contributions were quantified using coefficient weights estimated with the caret package (version 7.0-1). Larger absolute weights indicate a greater role in defining the separating hyperplane between classes.

In the k-nearest neighbors (kNN) model, all predictors were normalized prior to training using the class package to ensure equal scaling across features. The optimal number of neighbors (k) was selected via 10-fold repeated cross-validation. Classification was performed using majority voting among the nearest neighbors, with Euclidean distance.

The gradient boosting machine (GBM) model was built as an iterative ensemble of decision trees, where each successive tree aimed to reduce prediction error, using the gbm package (version 2.2.2). Hyperparameters, including the number of trees, depth, and learning rate, were optimized via repeated cross-validation. miRNA importance was derived from the cumulative contribution of each variable across all boosted trees.

MiRNA pathway analysis

To determine the biological pathways associated with the most influential cardiotoxicity-related miRNAs, enrichment analysis was carried out using DIANA-miRPath v4.0 (http://www.microrna.gr/miRPathv4, accessed on 19 July 2025). A combined selection strategy was used to refine candidates from both statistical and machine learning outputs. Only miRNAs that were significantly differentially expressed (FDR < 0.05) and ranked among the top 5 important features in at least one machine learning model were included in the final analysis.

Pathway annotation was performed using TarBase v8.1 as the interaction reference database and KEGG as the functional pathway source. The “pathways union” option was chosen to aggregate enrichment signals across all selected miRNAs. Statistical significance was determined using adjusted p-values, with a false discovery rate (FDR) threshold of < 0.05.

Statistical analysis

Continuous variables are summarized as mean ± standard deviation, whereas categorical variables are presented as percentages. The distribution of continuous data was examined using the Kolmogorov–Smirnov test together with probability–probability (P–P) plots. Differences between groups were evaluated using Student’s t-test for continuous outcomes and chi-square tests for categorical variables. For miRNA expression comparisons between cardiotoxicity and non-toxicity groups, t-tests were also applied.

To explore the prognostic relevance of individual miRNAs, we first ranked candidates by fold change. We selected the five most upregulated and the five most downregulated miRNAs observed between patients with and without cardiotoxicity. Each of these 10 miRNAs was then tested separately in univariate logistic regression models, with cardiotoxicity as the binary outcome and baseline-normalized miRNA levels as continuous predictors. Odds ratios (ORs), 95% confidence intervals (CIs), and corresponding p-values were derived for each model.

In parallel, receiver operating characteristic (ROC) curve analyses were performed for each selected miRNA to quantify their ability to distinguish between affected and unaffected patients. The area under the receiver operating characteristic (AUROC) and associated significance values were estimated for all 10 markers.

To compare predictive performance across machine learning methods, a one-way analysis of variance (ANOVA) was conducted with classification accuracy as the dependent variable and algorithm type as the grouping factor. Tukey’s Honestly Significant Difference (HSD) test was then applied for post hoc pairwise comparisons, allowing estimation of mean differences in accuracy between models along with adjusted p-values and 95% confidence intervals. All analyses were performed using RStudio version 2024.12.1.

Results and Discussion

Differential MiRNA expression

A cohort of 47 breast cancer patients was analyzed, among whom 15 individuals were classified in the cardiotoxicity subgroup. Baseline clinical and histopathological features for the entire population are detailed in **Table 1.** No statistically significant differences were identified between patients with and without cardiotoxicity with respect to age, tumor stage, radiotherapy exposure, prior medical history, smoking behavior, body mass

index, trastuzumab administration, or cumulative epirubicin dose. Notably, approximately 80% of participants presented with up to three involved lymph nodes and had received radiotherapy.

From the 84 miRNAs assessed, 45 showed significant expression differences between the cardiotoxic and non-cardiotoxic groups **(Figure 1).** Within these, 24 miRNAs were increased in the cardiotoxicity group, with the most pronounced fold changes observed for hsa-miR-17-5p, hsa-miR-22-3p, hsa-miR-145-5p, and hsa-miR-143-3p. The remaining miRNAs showed reduced expression in the cardiotoxicity group, with each exhibiting at least a twofold difference between cohorts. The strongest decreases were observed for hsa-miR-155-5p, hsa-miR-124-3p, and hsa-miR-133a-3p, with fold changes ranging from −4.7 to −3.87.

Based on fold-change magnitude, the top five upregulated miRNAs were hsa-miR-17-5p, hsa-miR-22-3p, hsa-miR-145-5p, hsa-miR-143-3p, and hsa-miR-21-5p. In contrast, the most strongly downregulated miRNAs included hsa-miR-155-5p, hsa-miR-124-3p, hsa-miR-133a-3p, hsa-miR-181a-5p, and hsa-miR-210-3p. These ten miRNAs were subsequently selected for downstream association testing. The hierarchical clustering displayed in the heatmap further supports the biological separation underlying the statistical patterns observed **(Figure 2).**

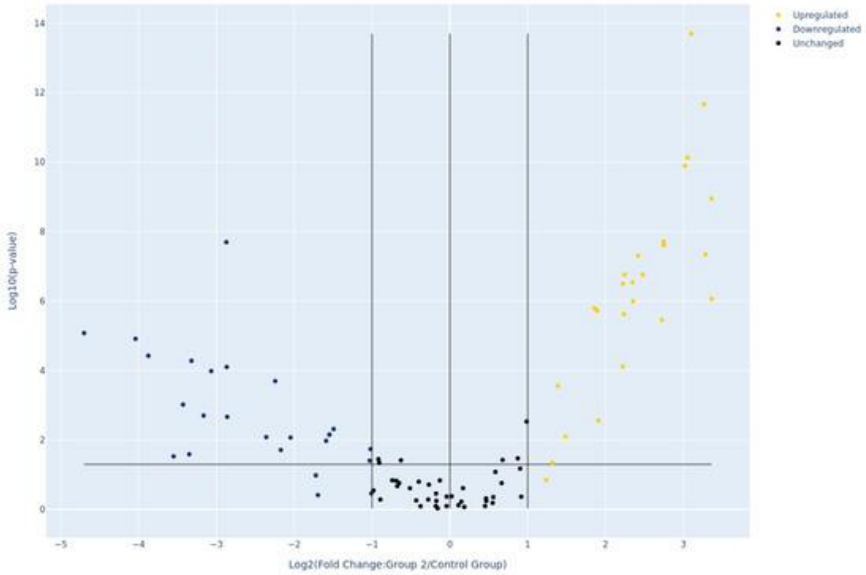

Figure 1. Volcano plot illustrating expression patterns of all 84 miRNAs analyzed. Red markers denote miRNAs meeting the thresholds of $-1 < \log2FC > 1$ (equivalent to at least a 2-fold change) and $-\log10p > 1.31$ ($P < 0.05$, Student's t-test).

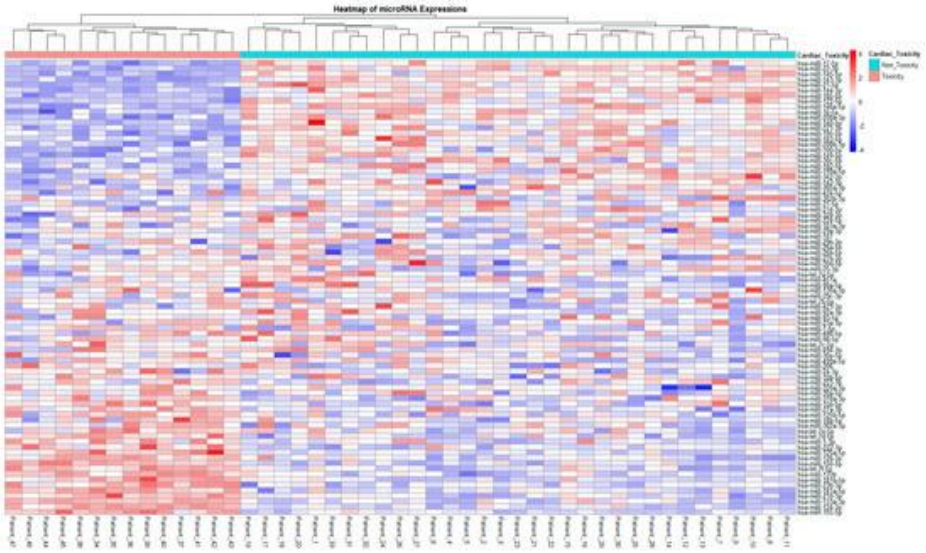

Figure 2. Heatmap representing standardized miRNA expression profiles across individuals with and without cardiotoxicity. Each column corresponds to a patient, while each row corresponds to a miRNA. Color scaling

reflects normalized expression levels (blue = decreased expression, red = increased expression). Samples are ordered according to cardiotoxicity status (left: cardiotoxicity, right: non-cardiotoxicity), and miRNAs are arranged by effect size (mean difference between groups) and clustered hierarchically according to overall expression similarity (fold change patterns).

Table 1. Clinical and histopathological characteristics of the 47 breast cancer patients.

Variables	P-value	Non-cardiac toxicity (n = 32)	Cardiac toxicity (n = 15)
Age (years)	0.88	56.3 ± 11.8	56.9 ± 12.9
Disease stage (pTNM)	0.80		
Stage I		14 (43.8)	8 (53.3)
Stage II		14 (43.8)	5 (33.3)
Stage III		4 (12.5)	2 (13.3)
Radiotherapy received	0.28	25 (78.1)	14 (93.3)
Systolic blood pressure (mmHg)	0.67	116 ± 18	119 ± 19
Diastolic blood pressure (mmHg)	0.73	80 ± 11	78 ± 13
Hypertension	0.51	11 (34.4)	4 (26.6)
Dyslipidemia	0.97	13 (40.6)	6 (39.9)
Diabetes mellitus	0.67	4 (12.5)	1 (6.6)
Non-smokers	0.91	21 (65.6)	10 (66.6)
Former smokers		6 (18.8)	2 (13.3)
Current smokers		5 (15.6)	3 (20)
Body mass index (kg/m²)	0.13	25.94 ± 4.59	28.13 ± 4.63
Trastuzumab therapy	0.34	27 (84.4)	11 (73.3)
Cumulative epirubicin dose (mg/m²)	0.97	516 ± 49	515 ± 51

Categorical variables are presented as N (%).
Continuous variables are presented as mean ± SD.

Association of Top deregulated miRNAs with cardiotoxicity

Among the five miRNAs showing the greatest downregulation, elevated baseline levels of hsa-miR-155-5p and hsa-miR-124-3p were significantly linked to the development of cardiotoxicity (OR = 1.12, 95% CI = 1.01–1.23, P = 0.03, and OR = 1.11, 95% CI = 1.01–1.24, P = 0.03, respectively) **(Table 2).** Meanwhile, hsa-miR-181a-5p and hsa-miR-210-3p from the same subset exhibited only borderline statistical associations with cardiotoxicity (both OR = 1.10, 95% CI = 0.99–1.22; P = 0.056 and 0.057, respectively).

Table 2. Univariate logistic regression and receiver operating characteristic (ROC) analyses evaluating associations between baseline expression of the top five upregulated and top five downregulated miRNAs and cardiotoxicity.

miR	P-value	AUROC	P-value	OR (95% CI)
hsa-miR-17-5p	0.047	0.69	0.16	0.92 (0.83–1.03)
hsa-miR-22-3p	0.06	0.68	0.15	0.92 (0.82–1.03)
hsa-miR-145-5p	0.041	0.69	0.19	0.93 (0.84–1.04)
hsa-miR-143-3p	0.037	0.69	0.19	0.93 (0.84–1.04)
hsa-miR-21-5p	0.045	0.69	0.20	0.93 (0.84–1.04)
hsa-miR-155-5p	0.006	0.76	0.03	1.12 (1.01–1.23)
hsa-miR-124-3p	0.007	0.75	0.03	1.11 (1.01–1.24)
hsa-miR-133a-3p	0.89	0.51	0.73	1.02 (0.92–1.12)
hsa-miR-181a-5p	0.008	0.75	0.056	1.10 (0.99–1.22)
hsa-miR-210-3p	0.025	0.71	0.057	1.10 (0.99–1.22)

ROC curve analysis showed modest discriminatory performance for the upregulated miRNA set **(Figure 3),** with AUROC values ranging from approximately 0.68 to 0.69. Within the downregulated group, hsa-miR-155-5p and hsa-miR-124-3p achieved the strongest classification performance, with AUROC values of 0.76 (P = 0.006) and 0.75 (P = 0.007), respectively.

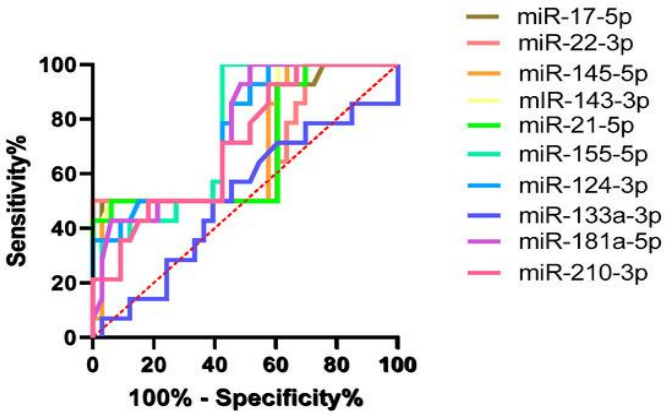

Figure 3. ROC curves depicting the ability of selected circulating microRNAs to differentiate patients who developed cardiotoxicity from those who remained unaffected. The vertical axis represents sensitivity (%), and the horizontal axis represents 100%- specificity (%). The red dashed diagonal line indicates the no-discrimination reference level (AUC = 0.5).

Machine learning models

The decision tree model comprised three sequential nodes and relied on two main splitting criteria to separate non-toxicity from cardiotoxicity cases. At the initial (root) split, classification depended on hsa-miR-17-5p expression (≥ 27 CT), which emerged as the strongest predictor. All samples meeting hsa-miR-17-5p ≥ 27 CT were assigned directly to the non-toxicity class with 100% certainty, comprising 41% of the dataset.

For the remaining samples with hsa-miR-17-5p < 27 CT, classification proceeded to a second decision point based on hsa-miR-185-5p levels. When hsa-miR-185-5p was ≥ 29 CT, the model predicted cardiotoxicity with full certainty, accounting for 51% of all cases. If hsa-miR-185-5p fell below 29 CT, samples were classified as non-toxicity, accounting for 8% of the cohort.

In addition, four alternative machine learning approaches (kNN, SVM, RF, and GBM) were evaluated. Their performance outcomes are presented in **Table 3**, where kNN, SVM, and RF demonstrated superior predictive strength. According to the SVM analysis, cardiotoxicity was linked to hsa-miR-143-3p, hsa-miR-133b, hsa-miR-145-5p, hsa-miR-185-5p, and hsa-miR-199a-5p **(Figure 4).** In contrast, the RF model highlighted hsa-miR-185-5p, hsa-miR-145-5p, hsa-miR-17-5p, hsa-miR-144-3p, and hsa-miR-133a-3p as the most relevant features **(Figure 5).** Overall, kNN, RF, and SVM consistently achieved better discrimination of cardiotoxicity compared with the decision tree model **(Table 4).**

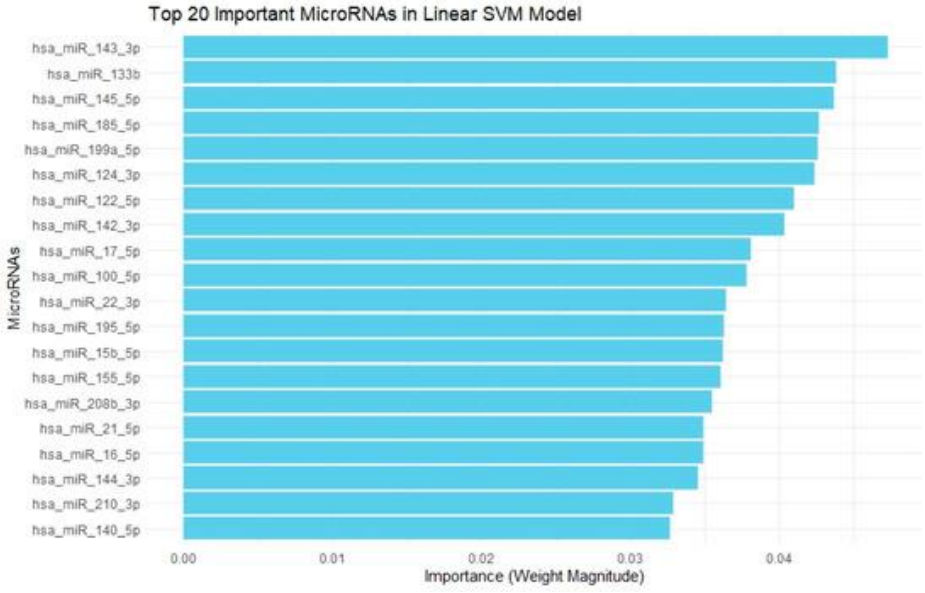

Figure 4. Ranking of the 20 most influential miRNAs related to chemotherapy-associated cardiotoxicity using a linear Support Vector Machine model. The bar plot shows feature importance derived from absolute

SVM weight coefficients. A greater weight magnitude indicates a stronger contribution to classification performance, with hsa-miR-143-3p showing the highest importance.

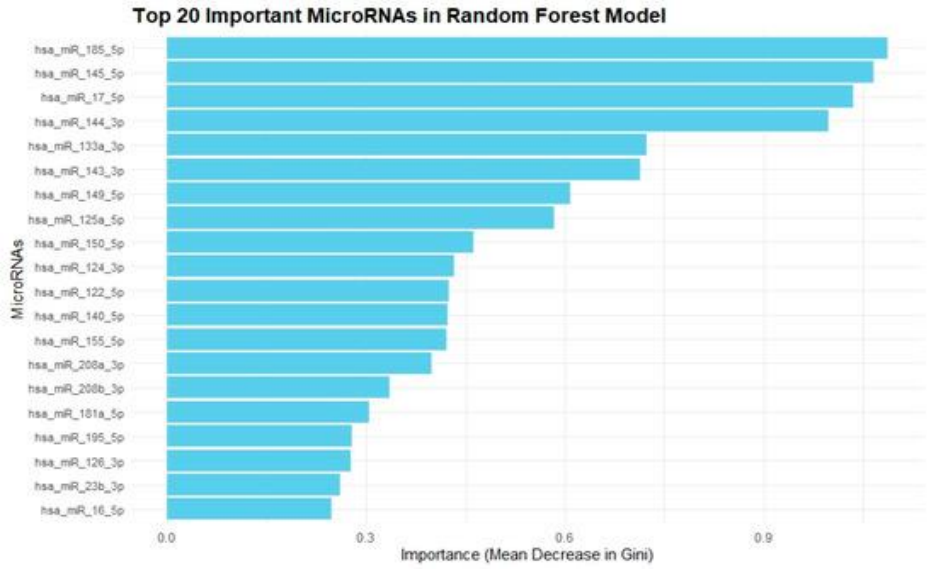

Figure 5. Top 20 miRNAs associated with chemotherapy-related cardiotoxicity identified using a Random Forest model. This visualization ranks features by the mean decrease in Gini impurity, with higher values indicating stronger predictive contribution. The most influential miRNA in this model is hsa-miR-185-5p.

Table 3. Performance metrics of machine learning models.

Machine learning model	Specificity	Sensitivity	Kappa	F1 score	Recall	Precision	Accuracy
k-nearest neighbors	0.88	0.83	1.00	0.88	0.87	0.88	0.89
Support vector machine	1	0.83	1.00	0.91	0.90	0.91	0.92
Random forest	0.88	0.83	1.00	0.90	0.89	0.90	0.91
Gradient boosting	0.88	1	0.64	0.92	0.91	0.92	0.93
Decision tree	1	0.50	0.50	0.67	0.50	1.00	0.75

Table 4. Comparative evaluation of the machine learning models.

Comparison	P-value	Mean difference in accuracy (95% CI)
GBM vs. Decision tree	0.13	0.18 (−0.04, 0.40)
kNN vs. Decision tree	0.045	0.22 (0.01, 0.44)
RF vs. Decision tree	0.03	0.24 (0.02, 0.45)
SVM vs. Decision tree	0.02	0.24 (0.03, 0.46)
kNN vs. GBM	0.98	0.04 (−0.18, 0.26)
RF vs. GBM	0.94	0.06 (−0.16, 0.27)
SVM vs. GBM	0.90	0.06 (−0.15, 0.28)
RF vs. kNN	0.99	0.02 (−0.20, 0.23)
SVM vs. kNN	0.99	0.02 (−0.19, 0.24)
SVM vs. RF	0.99	0.01 (−0.21, 0.23)

Pathway analysis

Pathway enrichment results revealed that the most significantly overrepresented pathways were "Proteoglycans in cancer" (FDR = 1.3×10^{-13}), "Focal adhesion" (FDR = 5.9×10^{-12}), "Shigellosis" (FDR = 8.2×10^{-12}), "p53 signaling pathway" (FDR = 2.7×10^{-11}), and "Salmonella infection" (FDR = 3.6×10^{-11}). Additional highly significant pathways included "MAPK signaling pathway," "Pathways in cancer," and "Apoptosis," all exhibiting FDR values below 1×10^{-8}. **Figure 6** presents a bar chart of the top 10 enriched pathways ranked by –log10(FDR). Among all analyzed miRNAs, hsa-miR-17-5p showed the widest involvement across pathways, followed by hsa-miR-145-5p and hsa-miR-143-3p. The number of pathways linked to individual miRNAs ranged from 2 to 10,

reflecting variability in network connectivity and signaling process overlap. Meanwhile, the number of genes mapped per pathway ranged from 8 to 54, depending on pathway complexity and miRNA coverage.

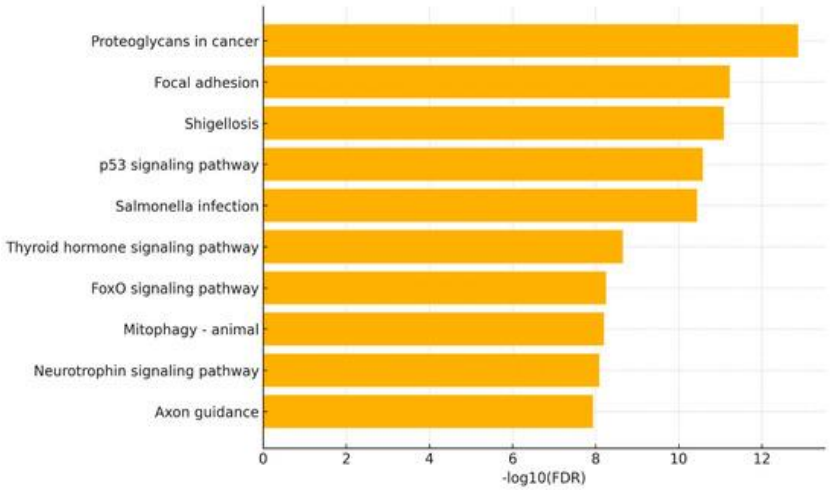

Figure 6. Pathway enrichment analysis performed using DIANA-miRPath v4.0. Target interactions were retrieved from TarBase v8.1, and functional annotation was based on KEGG pathways. Enrichment analysis employed the "pathways union" approach to capture combined effects across all miRNAs. Statistical significance was evaluated using adjusted p-values (false discovery rate (FDR) < 0.05). The most significantly enriched pathways included "Proteoglycans in cancer" (FDR = 1.3×10^{-13}), "Focal adhesion" (FDR = 5.9×10^{-12}), "Shigellosis" (FDR = 8.2×10^{-12}), "p53 signaling pathway" (FDR = 2.7×10^{-11}), and "Salmonella infection" (FDR = 3.6×10^{-11}).

Despite the recognized need for reliable prognostic biomarkers in cardiotoxicity induced by anticancer therapies, currently available cardiac biomarkers remain insufficient, as they do not provide adequate predictive accuracy in terms of sensitivity and specificity. MicroRNAs (miRNAs) are small, single-stranded, non-coding RNA molecules of approximately 18–25 nucleotides that regulate gene expression and are involved in key biological processes such as differentiation, apoptosis, and cell death [17]. A wide range of miRNAs has been associated with cardiac disorders, including heart failure (miR-18a-5p, miR-26b-5p, miR-27a-3p, miR-30e-5p, miR-106a-5p, miR-199a-3p, and miR-652-3p) [18] and acute myocardial infarction (miR-1, miR-21, miR-29a, miR-133a, and miR-208) [19, 20].

In this investigation, 84 baseline miRNAs were analyzed as candidate prognostic biomarkers for cardiotoxicity induced by anthracycline and trastuzumab treatment. The selection of the Human Cardiovascular Disease Focus V2 panel is supported by strong prior evidence linking these miRNAs to cardiovascular disease mechanisms, organ specificity, and biomarker relevance. Several miRNAs (let-7, miR-1, miR-133, miR-208, miR-126, miR-145, and miR-155) play fundamental roles in cardiac development, myocardial remodeling, vascular regulation, and angiogenesis.

Our results showed that hsa-miR-17-5p, hsa-miR-22-3p, hsa-miR-145-5p, and hsa-miR-143-3p were significantly upregulated, each by at least 9-fold, whereas hsa-miR-155-5p, hsa-miR-124-3p, and hsa-miR-133a-3p were strongly downregulated, with reductions exceeding 14-fold. Previous studies evaluating miRNA signatures in anthracycline- and trastuzumab-associated cardiotoxicity have reported alterations in more than 400 miRNAs, with some showing increased and others decreased expression [21-29]. This extensive heterogeneity reflects the multiple biological mechanisms and signaling cascades involved in treatment-related cardiac injury.

Importantly, our findings align partially with a recent pilot study, as both investigations evaluated let-7f-5p, miR-1-3p, and miR-126-3p and reported significant baseline differences for these three miRNAs [30]. Nevertheless, directionality differences were observed for miR-126-3p: in our cohort, baseline levels were reduced in patients who later developed cardiotoxicity, whereas Pivatto Junior *et al*. reported elevated baseline expression in the same group. Moreover, the reduced baseline expression of let-7f-5p and miR-1-3p observed in our study was not reproduced in the pilot dataset.

Pathway enrichment analysis of the most influential miRNAs further demonstrated significant involvement in signaling pathways associated with cardiotoxic mechanisms. The most significantly enriched pathways included

focal adhesion, p53 signaling, apoptosis, and MAPK signaling, all of which are known to participate in myocardial injury, cell death, and structural remodeling during chemotherapy exposure. The repeated presence of miR-17-5p, miR-145-5p, and miR-143-3p across these pathways suggests that these miRNAs may act as central regulatory nodes.

Interestingly, infection-related pathways such as Shigellosis and Salmonella infection were also significantly enriched; however, this likely reflects shared inflammatory and apoptosis-related signaling rather than true infectious mechanisms. Collectively, these pathway alterations correspond to established mechanisms of chemotherapy-related cardiotoxicity, including DNA damage triggered by anthracyclines, p53-mediated apoptotic activation, oxidative and mitochondrial stress, disruption of cytoskeletal and focal adhesion structures, and maladaptive MAPK-driven hypertrophic and fibrotic remodeling.

Among previously reported miRNAs linked to anthracycline- and trastuzumab-induced cardiotoxicity, miR-133, miR-1, miR-21, miR-34a, miR-30e, and miR-222-3p have been most consistently implicated [22, 25-28, 31]. Several clinical studies have evaluated temporal dynamics of miRNA expression at different time intervals after therapy initiation, including every 3 months [28], every 15 days [29], and every 3 weeks [22]. The most frequently used monitoring schedule was every 3 months during the first 6 months of treatment. However, variation in sampling timepoints likely contributes to inconsistencies in miRNA associations across studies.

Recognizing the limitations of single-biomarker approaches, we developed a decision tree model to provide an interpretable classification framework based on miRNA expression thresholds. This model enables straightforward clinical interpretation for distinguishing cardiotoxic from non-cardiotoxic outcomes. The primary splitting variable was miR-17-5p, identified as the most informative predictor, followed by miR-185-5p in cases with low miR-17-5p expression.

This structure highlights the potential of miRNA signatures as practical tools for cardiotoxicity classification. miR-17-5p has previously been implicated in anthracycline-related cardiotoxicity in both experimental and clinical settings, although findings remain inconsistent [32, 33]. Likewise, while the direct role of miR-185-5p in chemotherapy-induced cardiotoxicity is not yet clearly defined, it has been associated with cardiac processes such as myocardial fibrosis and angiogenesis, suggesting an indirect contribution to cardiotoxic mechanisms [34, 35].

Across four additional machine learning approaches, distinct miRNAs emerged as dominant contributors to cardiotoxicity prediction. In the Random Forest (RF) model, hsa-miR-185-5p showed the strongest association with cardiac toxicity, whereas hsa-miR-145-5p and hsa-miR-143-3p were the leading features in the GBM and linear SVM models, respectively. Importantly, hsa-miR-145-5p and hsa-miR-143-3p were repeatedly ranked among the most influential variables across all applied algorithms, indicating a high degree of consistency in their predictive relevance. Notably, the miRNAs most strongly linked to cardiotoxicity in the machine-learning framework were also clustered in the same region of the heatmap, supporting their shared expression pattern.

In terms of performance, all four machine learning models demonstrated superior predictive accuracy compared with the decision tree. While the decision tree offers greater interpretability and may be considered suitable for simplified clinical decision support, its reduced predictive performance highlights a clear trade-off between interpretability and accuracy. Nevertheless, translation into clinical practice requires additional steps, including external validation in independent cohorts, development of user-friendly software tools, and harmonization of miRNA quantification methods. Ultimately, miRNA-based machine learning models will only achieve clinical utility if implemented within standardized, reproducible, and cost-effective frameworks.

Beyond machine learning approaches, logistic regression combined with ROC analysis identified hsa-miR-155-5p and hsa-miR-124-3p as significant discriminative biomarkers. To reduce bias from repeated measurements, this analysis was restricted to the most differentially expressed miRNAs. However, the miRNAs highlighted through ROC analysis differed from those selected by machine learning models. This discrepancy should be interpreted cautiously, as ROC-based single-marker evaluation is more susceptible to measurement variability and prior feature selection bias. In contrast, machine learning methods integrate multiple variables simultaneously and are therefore less influenced by fluctuations in individual markers. Consequently, machine learning approaches may provide a more robust framework for interpreting miRNA expression data, although further validation remains necessary.

All miRNAs identified in this study have been previously associated with biological mechanisms relevant to cardiotoxicity. Specifically, hsa-miR-185-5p is involved in myocardial fibrosis, angiogenesis, and apoptosis regulation, while hsa-miR-143-3p modulates the AKT signaling pathway, both of which are closely linked to cardiotoxic processes [34-36]. In addition, hsa-miR-145-5p and hsa-miR-155-5p have been reported to be

upregulated in cardiomyocytes following doxorubicin exposure [37], whereas hsa-miR-17-5p has been associated with anthracycline-induced cardiotoxicity in both experimental and clinical studies, albeit with inconsistent findings [32, 33, 37]. In contrast, hsa-miR-124 appears to exert a protective role by reducing oxidative stress and limiting apoptosis and autophagy in response to chemotherapy [38, 39]. Moreover, levels of hsa-miR-22-3p [40] and hsa-miR-133a-3p [41] are significantly decreased in cardiomyocytes exposed to anthracyclines.

A substantial proportion of these miRNAs is also implicated in breast cancer biology. In particular, hsa-miR-185-5p, hsa-miR-143-3p, hsa-miR-145-5p, hsa-miR-124, hsa-miR-22-3p, and hsa-miR-133a-3p are generally downregulated in breast cancer and are considered tumor suppressor miRNAs, whereas hsa-miR-155-5p and hsa-miR-17-5p are typically characterized as oncogenic. Functionally, hsa-miR-185-5p regulates epithelial–mesenchymal transition (EMT) and breast cancer cell invasion through targeting the receptor for advanced glycation end-products (RAGE) [42]. At the same time, hsa-miR-143-3p suppresses the RAS/MEK/ERK and PI3K/AKT/mTOR signaling cascades, both of which are essential components of HER2 downstream signaling [43]. Based on their functional roles and expression patterns observed in this study, hsa-miR-185-5p, hsa-miR-143-3p, and hsa-miR-145-5p emerged as the most consistently replicated and biologically plausible candidates across all machine learning models. In contrast, hsa-miR-17-5p, hsa-miR-124, and hsa-miR-133a-3p showed less stable predictive behavior or contradictory patterns, reducing their suitability as standalone biomarkers. Overall, the consistent involvement of hsa-miR-185-5p, hsa-miR-143-3p, and hsa-miR-145-5p supports their potential as key biomarker candidates requiring further validation in future studies.

HER2 overexpression in HER2-positive breast cancer is associated with distinct miRNA expression profiles compared with HER2-negative tumors, and specific alterations have also been reported in relation to HER2 genotypic variation. For instance, hsa-miR-33b is markedly downregulated in HER2-positive tumors, where it targets MYC and suppresses EZH2 expression [44]. In contrast, hsa-miR-21 activates the RAS/MEK/ERK signaling cascade, a key downstream pathway of HER2 signaling in breast cancer cells [45]. Additionally, hsa-miR-4728 is encoded within an intronic region of the HER2 gene and is co-expressed with HER2 overexpression, acting by regulating EBP1 and ESR1 [46, 47]. Furthermore, the aggressive p95HER2 variant is characterized by increased expression of hsa-miR-221, hsa-miR-222, and hsa-miR-503, which together form a distinct miRNA signature [48].

Despite the biological relevance of the miRNAs identified in this study, existing literature does not provide strong evidence linking them to specific HER2 molecular subtypes or levels of HER2 overexpression. In addition, our dataset did not enable a direct evaluation of relationships between HER2 status (including IHC staining intensity or mRNA expression) and circulating miRNA profiles, which constitutes a major limitation of this work. Future investigations should therefore include larger, well-characterized patient populations and incorporate comprehensive HER2 molecular profiling—such as IHC scoring, FISH analysis, and transcriptomic quantification. This level of stratification may help uncover subtype-dependent miRNA signatures and enhance the precision of cardiotoxicity risk prediction in HER2-positive breast cancer patients.

Several additional limitations should also be acknowledged. First, miRNA measurements were restricted to baseline, with no longitudinal sampling across treatment time points, limiting insight into temporal dynamics. Second, the relatively small number of patients who developed cardiotoxic events reduces statistical robustness and limits the reliability of classical regression-based inference. Third, the overall cohort size was modest, thereby inherently constraining statistical power and increasing susceptibility to random variation.

Moreover, multiple pre-analytical and technical factors may have influenced miRNA quantification. These include inter-individual variability in baseline cardiac status, differences in sample handling time, and potential batch effects during RNA extraction and qPCR processing. Additional variability may arise from pre-analytical procedures such as plasma separation timing and storage conditions. Furthermore, the lack of standardized protocols for miRNA quantification and normalization remains a key obstacle for their clinical application as prognostic tools. Although alternative strategies, such as self-referencing miRNA pairs, could improve normalization robustness by avoiding reliance on housekeeping controls, these approaches require substantially larger datasets for training and validation and were not feasible within the scope of this exploratory study.

In addition, the study design does not allow attribution of cardiotoxic effects to a specific chemotherapeutic agent; therefore, a direct causal link between individual miRNAs and anthracycline- or trastuzumab-related toxicity cannot be established. The identified miRNA signatures also lack external validation in independent cohorts, which further limits the generalizability and robustness of the findings. Finally, the use of synthetic data balancing techniques may have introduced additional bias into the analytical pipeline.

Building on these preliminary results, future research should focus on reducing the miRNA panel through pathway-driven selection and on integrating artificial intelligence–based analytical frameworks. Large-scale, prospective, randomized studies including well-defined cohorts receiving anthracyclines and/or trastuzumab, together with standardized miRNA measurement protocols, are required to validate the prognostic value of these candidate biomarkers.

Conclusion

This work demonstrates the potential of circulating miRNAs as predictive biomarkers for therapy-related cardiotoxicity in HER2-positive breast cancer patients. Among the 84 miRNAs analyzed, multiple transcripts showed clear expression differences between patients who developed cardiotoxicity and those who did not. Notably, miR-185-5p, miR-145-5p, and miR-143-3p were consistently ranked among the top-performing predictors across different machine learning approaches, supporting their relevance for risk classification. Additionally, ROC analysis identified hsa-miR-155-5p and hsa-miR-124-3p as markers with moderate discriminative capability. Overall, machine learning models—particularly SVM, kNN, and RF—achieved higher predictive performance than traditional decision tree methods, emphasizing the benefit of more advanced computational strategies in miRNA-based risk prediction. These findings support the concept that combining circulating miRNA profiling with AI-driven analytical frameworks may enable earlier identification of patients at increased risk and facilitate personalized monitoring and intervention strategies. However, confirmation in larger, prospective, longitudinal studies with standardized laboratory protocols is required before clinical implementation of these miRNA-based predictive models.

Acknowledgments: None

Conflict of Interest: None

Financial Support: This study was funded by Hellenic Society of Medical Oncology (HeSMO), Greece (Grant No. 8019), and Hellenic Society of Cancer Markers and Targeted Therapy, Greece (Grant No. 6214).

Ethics Statement: Ethical approval for the study was obtained from the Ethics Committee of “Hippokration” Athens General Hospital (Approval Code: 8028; Approval Date: 17 June 2015).

References

1. Cardinale D, Colombo A, Bacchiani G, Tedeschi I, Meroni CA, Veglia F, et al. Early detection of anthracycline cardiotoxicity and improvement with heart failure therapy. Circulation. 2015;131:1981-8.
2. Farolfi A, Melegari E, Aquilina M, Scarpi E, Ibrahim T, Maltoni R, et al. Trastuzumab-induced cardiotoxicity in early breast cancer patients: A retrospective study of possible risk and protective factors. Heart. 2013;99:634-9.
3. Slamon DJ, Leyland-Jones B, Shak S, Fuchs H, Paton V, Bajamonde A, et al. Use of chemotherapy plus a monoclonal antibody against HER2 for metastatic breast cancer that overexpresses HER2. N Engl J Med. 2001;344:783-92.
4. Advani PP, Ballman KV, Dockter TJ, Colon-Otero G, Perez EA. Long-term cardiac safety analysis of NCCTG N9831 (Alliance) adjuvant trastuzumab trial. J Clin Oncol. 2016;34:581-7.
5. de Azambuja E, Procter MJ, van Veldhuisen DJ, Agbor-Tarh D, Metzger-Filho O, Steinseifer J, et al. Trastuzumab-associated cardiac events at 8 years of median follow-up in the Herceptin Adjuvant trial (BIG 1-01). J Clin Oncol. 2014;32:2159-65.
6. Cameron D, Piccart-Gebhart MJ, Gelber RD, Procter M, Goldhirsch A, de Azambuja E, et al. 11 years' follow-up of trastuzumab after adjuvant chemotherapy in HER2-positive early breast cancer: Final analysis of the HERceptin Adjuvant (HERA) trial. Lancet. 2017;389:1195-205.
7. Venkatesh P, Kasi A. Anthracyclines. In: StatPearls [Internet]. Treasure Island (FL): StatPearls Publishing; 2025. NBK538187.
8. Vogelsang TW, Jensen RJ, Hesse B, Kjaer A. BNP cannot replace gated equilibrium radionuclide ventriculography in monitoring of anthracycline-induced cardiotoxicity. Int J Cardiol. 2008;124:193-7.

9. Pavo N, Raderer M, Hulsmann M, Neuhold S, Adlbrecht C, Strunk G, et al. Cardiovascular biomarkers in patients with cancer and their association with all-cause mortality. Heart. 2015;101:1874-80.
10. Mathew P, Suarez W, Kip K, Bayar E, Jasty R, Matloub Y, et al. Is there a potential role for serum cardiac troponin I as a marker for myocardial dysfunction in pediatric patients receiving anthracycline-based therapy? A pilot study. Cancer Invest. 2001;19:352-9.
11. Zardavas D, Suter TM, Van Veldhuisen DJ, Steinseifer J, Noe J, Lauer S, et al. Role of troponins I and T and N-terminal prohormone of brain natriuretic peptide in monitoring cardiac safety of patients with early-stage human epidermal growth factor receptor 2-positive breast cancer receiving trastuzumab: A Herceptin Adjuvant Study cardiac marker substudy. J Clin Oncol. 2017;35:878-84.
12. Michel L, Mincu RI, Mahabadi AA, Settelmeier S, Al-Rashid F, Rassaf T, et al. Troponins and brain natriuretic peptides for the prediction of cardiotoxicity in cancer patients: A meta-analysis. Eur J Heart Fail. 2020;22:350-61.
13. Hinrichs L, Mrotzek SM, Mincu RI, Pohl J, Roll A, Michel L, et al. Troponins and natriuretic peptides in cardio-oncology patients: Data from the ECoR Registry. Front Pharmacol. 2020;11:740.
14. Cardinale D, Sandri MT, Colombo A, Colombo N, Boeri M, Lamantia G, et al. Prognostic value of troponin I in cardiac risk stratification of cancer patients undergoing high-dose chemotherapy. Circulation. 2004;109:2749-54.
15. Newie I, Sokilde R, Persson H, Grabau D, Rego N, Kvist A, et al. The HER2-encoded miR-4728-3p regulates ESR1 through a non-canonical internal seed interaction. PLoS One. 2014;9:e97200.
16. Yin C, Zhang G, Sun R, Pan X, Wang X, Li H, et al. miR-185-5p inhibits F-actin polymerization and reverses epithelial mesenchymal transition of human breast cancer cells by modulating RAGE. Mol Med Rep. 2018;18:2621-30.
17. Bartel DP. MicroRNAs: Genomics, biogenesis, mechanism, and function. Cell. 2004;116:281-97.
18. Lyon AR, Lopez-Fernandez T, Couch LS, Asteggiano R, Aznar MC, Bergler-Klein J, et al. 2022 ESC Guidelines on cardio-oncology developed in collaboration with the European Hematology Association (EHA), the European Society for Therapeutic Radiology and Oncology (ESTRO) and the International Cardio-Oncology Society (IC-OS). Eur Heart J Cardiovasc Imaging. 2022;23:e333-e465.
19. Pliakou E, Lampropoulou DI, Dovrolis N, Chrysikos D, Filippou D, Papadimitriou C, et al. Circulating miRNA expression profiles and machine learning models in association with response to irinotecan-based treatment in metastatic colorectal cancer. Int J Mol Sci. 2022;24:46.
20. Ovchinnikova ES, Schmitter D, Vegter EL, ter Maaten JM, Valente MAE, Liu LCY, et al. Signature of circulating microRNAs in patients with acute heart failure. Eur J Heart Fail. 2016;18:414-23.
21. Cheng M, Yang J, Zhao X, Zhang E, Zeng Q, Yu Y, et al. Circulating myocardial microRNAs from infarcted hearts are carried in exosomes and mobilise bone marrow progenitor cells. Nat Commun. 2019;10:959.
22. Zile MR, Mehurg SM, Arroyo JE, Stroud RE, DeSantis SM, Spinale FG. Relationship between the temporal profile of plasma microRNA and left ventricular remodeling in patients after myocardial infarction. Circ Cardiovasc Genet. 2011;4:614-9.
23. Yadi W, Shurui C, Tong Z, Suxian C, Qing T, Dongning H. Bioinformatic analysis of peripheral blood miRNA of breast cancer patients in relation with anthracycline cardiotoxicity. BMC Cardiovasc Disord. 2020;20:43.
24. Rigaud VO, Ferreira LR, Ayub-Ferreira SM, Avila MS, Brandao SM, Cruz FD, et al. Circulating miR-1 as a potential biomarker of doxorubicin-induced cardiotoxicity in breast cancer patients. Oncotarget. 2017;8:6994-7002.
25. Ruggeri C, Gioffre S, Achilli F, Colombo GI, D'Alessandra Y. Role of microRNAs in doxorubicin-induced cardiotoxicity: An overview of preclinical models and cancer patients. Heart Fail Rev. 2018;23:109-22.
26. Gioffre S, Chiesa M, Cardinale DM, Ricci V, Vavassori C, Cipolla CM, et al. Circulating microRNAs as potential predictors of anthracycline-induced troponin elevation in breast cancer patients: Diverging effects of doxorubicin and epirubicin. J Clin Med. 2020;9:1418.
27. Zhang S, Wang Y, Wang Y, Peng J, Yuan C, Zhou L, et al. Serum miR-222-3p as a double-edged sword in predicting efficacy and trastuzumab-induced cardiotoxicity for HER2-positive breast cancer patients receiving neoadjuvant target therapy. Front Oncol. 2020;10:631.

28. Feng Q, Ren Y, Hou A, Guo J, Mao Z, Liu S, et al. MicroRNA-130a increases and predicts cardiotoxicity during adjuvant chemotherapy in human epidermal growth factor receptor-2-positive breast cancer. J Breast Cancer. 2021;24:153-63.
29. Lakhani HV, Pillai SS, Zehra M, Dao B, Tirona MT, Thompson E, et al. Detecting early onset of anthracyclines-induced cardiotoxicity using a novel panel of biomarkers in West Virginian population with breast cancer. Sci Rep. 2021;11:7954.
30. Pillai SS, Pereira DG, Bonsu G, Chaudhry H, Puri N, Lakhani HV, et al. Biomarker panel for early screening of trastuzumab-induced cardiotoxicity among breast cancer patients in West Virginia. Front Pharmacol. 2022;13:953178.
31. Pizzamiglio S, Ciniselli CM, de Azambuja E, Agbor-Tarh D, Moreno-Aspitia A, Suter TM, et al. Circulating microRNAs and therapy-associated cardiac events in HER2-positive breast cancer patients: An exploratory analysis from NeoALTTO. Breast Cancer Res Treat. 2024;206:285-94.
32. Pivatto Junior F, Santos ABS, Englert EF, Mazzutti G, Costa GOM, Saffi MAL, et al. MicroRNA expression pre-trastuzumab treatment in HER-2-positive early breast cancer patients as a predictor of cancer therapy-related cardiac dysfunction: A pilot cohort study. Cardiology. 2025;1-8.
33. Alexandraki A, Papageorgiou E, Zacharia M, Keramida K, Papakonstantinou A, Cipolla CM, et al. New insights in the era of clinical biomarkers as potential predictors of systemic therapy-induced cardiotoxicity in women with breast cancer: A systematic review. Cancers (Basel). 2023;15:3290.
34. Qin X, Chang F, Wang Z, Jiang W. Correlation of circulating pro-angiogenic miRNAs with cardiotoxicity induced by epirubicin/cyclophosphamide followed by docetaxel in patients with breast cancer. Cancer Biomark. 2018;23:473-84.
35. Wan G, Chen P, Sun X, Cai X, Yu X, Wang X, et al. Weighted gene co-expression network-based approach to identify key genes associated with anthracycline-induced cardiotoxicity and construction of miRNA-transcription factor-gene regulatory network. Mol Med. 2021;27:142.
36. Li CC, Qiu XT, Sun Q, Zhou JP, Yang HJ, Wu WZ, et al. Endogenous reduction of miR-185 accelerates cardiac function recovery in mice following myocardial infarction via targeting of cathepsin K. J Cell Mol Med. 2019;23:1164-73.
37. Lin R, Rahtu-Korpela L, Szabo Z, Kemppi A, Skarp S, Kiviniemi AM, et al. MiR-185-5p regulates the development of myocardial fibrosis. J Mol Cell Cardiol. 2022;165:130-40.
38. Degerli E, Torun V, Cansaran-Duman D. miR-185-5p response to usnic acid suppresses proliferation and regulating apoptosis in breast cancer cell by targeting Bcl2. Biol Res. 2020;53:19.
39. Chen Y, Xu Y, Deng Z, Wang Y, Zheng Y, Jiang W, et al. MicroRNA expression profiling involved in doxorubicin-induced cardiotoxicity using high-throughput deep-sequencing analysis. Oncol Lett. 2021;22:560.
40. Zhang X, Liu F, Wang Q, Geng Y. Overexpressed microRNA-506 and microRNA-124 alleviate H2O2-induced human cardiomyocyte dysfunction by targeting kruppel-like factor 4/5. Mol Med Rep. 2017;16:5363-9.
41. Liu Y, Li Y, Ni J, Shu Y, Wang H, Hu T. MiR-124 attenuates doxorubicin-induced cardiac injury via inhibiting p66Shc-mediated oxidative stress. Biochem Biophys Res Commun. 2020;521:420-6.
42. Rosenfeld R, Riondino S, Formica V, Torino F, Martuscelli E, Roselli M. MiRNAs and circRNAs for the diagnosis of anthracycline-induced cardiotoxicity in breast cancer patients: A narrative review. J Pers Med. 2022;12:1059.
43. Chen L, Xu Y. MicroRNAs as biomarkers and therapeutic targets in doxorubicin-induced cardiomyopathy: A review. Front Cardiovasc Med. 2021;8:740515.
44. Gorbatenko A, Sokilde R, Sorensen EE, Newie I, Persson H, Morancho B, et al. HER2 and p95HER2 differentially regulate miRNA expression in MCF-7 breast cancer cells and downregulate MYB proteins through miR-221/222 and miR-503. Sci Rep. 2019;9:3352.
45. Haryana SM, Oktriani R, Faiha DK, Conara FC, Dafip M, Setiasari DW. miR-143-3p: a critical regulator of KRAS and HRAS with potential for targeted therapies in breast cancer. Trends Sci. 2025;22:9630.
46. Zhou Y, Yuan Y, Li L, Wang X, Quan Y, Liu C, et al. HER2-intronic miR-4728-5p facilitates HER2 expression and accelerates cell proliferation and migration by targeting EBP1 in breast cancer. PLoS One. 2021;16:e0245832.

47. Pattanayak B, Garrido-Cano I, Adam-Artigues A, Tormo E, Pineda B, Cabello P, et al. MicroRNA-33b suppresses epithelial-mesenchymal transition repressing the MYC-EZH2 pathway in HER2+ breast carcinoma. Front Oncol. 2020;10:1661.
48. Huang TH, Wu F, Loeb GB, Hsu R, Heidersbach A, Brincat A, et al. Up-regulation of miR-21 by HER2/neu signaling promotes cell invasion. J Biol Chem. 2009;284:18515-24.